



CONTINUOUS ADSORPTION OF METHYLENE BLUE DYE ON THE MAIZE STEM GROUND TISSUE

*Predrag S. Kojić**, *Vesna V. Vučurović*, *Nataša Lj. Lukić*, *Milica Ž. Karadžić*,
Svetlana S. Popović

University of Novi Sad, Faculty of Technology Novi Sad, Bulevar Cara Lazara 1, 21000 Novi Sad, Serbia

Continuous adsorption of methylene blue from aqueous solutions onto maize stem ground tissue in column mode was investigated. The study encompassed the effects of important parameters such as flow rate, initial concentration of methylene blue, and bed depth on methylene blue removal from model solutions. The maximum adsorption capacity of the maize stem was 45.9 mg/g at the initial methylene blue concentration of 20 mg/L, bed height of 6.5 cm and flow rate of 8 mL/min. It was found that the breakthrough time for reaching saturation increased with a decrease in the flow rate, and also occurred earlier for a higher influent concentration. The breakthrough times increased with the bed depth, thus allowing a larger volume to be treated. The Adams-Bohart, Yoon-Nelson, Clark and artificial neural network models were used to predict the breakthrough curves. These models gave excellent approximations of the experimental behavior.

KEY WORDS: biosorption, fixed-bed column, breakthrough curve, maize stem, modeling, ANN

INTRODUCTION

Many industries, such as paper making, plastics, food, cosmetics, textile, etc., use dyes in order to color their products. The presence of these dyes in water, even at very low concentrations, is highly visible and undesirable (1). Adsorption is one of the processes that used for dye removal in wastewater treatment (2). Activated carbon is the most widely used adsorbent because it has excellent adsorption efficiency for organic compounds, but its use is usually limited due to high costs (3). This method will become less expensive if the adsorbent is made from cheap and easily available materials.

Methylene blue (MB) was extensively used as the model adsorbate in the previous studies (3-10). The MB is a thiazine (cationic) dye that is generally used for dyeing cotton, coloring paper, wool, silk, hair, etc. Though MB is not strongly hazardous, it can cause some harmful effects (7).

The search for a low cost and easily available adsorbent led to the investigation of materials of agricultural and biological origin, along with industrial by-products, as ad-

* Corresponding author: Predrag S. Kojić, University of Novi Sad, Faculty of Technology Novi Sad, Bulevar Cara Lazara 1, 21000 Novi Sad, Serbia, e-mail: kojic@tf.uns.ac.rs



sorbents (11). In the recent years, many researchers have proved several low cost materials for the removal of MB from its aqueous solutions, such as wheat shells (12), chaff (8), Indian Rosewood sawdust (3), phoenix tree leaf powder (9), rice husk (1, 7), Neem leaf powder (13). The list of numerous adsorbents for MB removal were presented by Ralatullah et al. (10). Bhatnagar et al. (14) reported a review of agro-industrial and municipal waste materials as potential adsorbents for water treatment.

In the present study, maize stem ground tissue has been used as an adsorbent for the removal of MB from its aqueous solutions. The material is extremely cheap, non-toxic, chemically inert and easily available biodegradable waste. To our knowledge, this is the first study about dye adsorption on this adsorbent in the column mode.

The aim of this work was to promote our previous study (15) on the development of a convenient and economic method for MB removal on maize stem grand tissue as a low-cost and easily available biodegradable adsorbent. The effect of adsorptive time, flow rate, MB concentration, and bed depth on MB removal from aqueous solutions in the column mode was investigated. The Adams-Bohart, Yoon-Nelson, Clark and artificial neural network models were used to predict the breakthrough curves.

EXPERIMENTAL

Preparation of the adsorbent

Maize stems of Gold Cup maize hybrid were collected from ready-to-harvest maize fields from Budisava, Serbia. The details on the preparation and characterization of the adsorbent can be found in the our previous paper (15).

Preparation of the MB solutions

All of the MB solutions were prepared with distilled water. Three different concentrations of the MB solutions were prepared and used in this work: 5 mg/L, 10 mg/L and 20 mg/L.

Experimental methods

A known adsorbent mass of 0.35, 0.45 and 0.65 g was packed into a plastic column of 1.2 cm internal diameter and 10 cm in height, to achieve a bed depth of 3.5, 4.5 and 6.5 cm, respectively. The column was operated in a downflow mode using gravity force. Three different influent flow rates were used: 8 mL/min, 20 mL/min and 40 mL/min. Flow rate was regulated by a valve located above the column.

Samples of the effluent (10 mL aliquot) were collected at regular intervals. Concentrations of MB in the samples were determined spectrophotometrically on a SECOMAM Prim: Light and Advance spectrophotometer, in the visible range of the spectrum. Distilled water was used as the reference sample. The maximum absorbance wavelength was 668 nm.



Fixed bed column adsorption studies

The performance of the column was described through the concept of the breakthrough curve. The breakthrough curve is expressed in terms of a normalized concentration defined as the ratio of the outlet to inlet MB concentration (C/C_0) as a function of time or volume effluent.

The effluent volume (V_{eff}) was calculated as:

$$V_{\text{eff}} = Qt_{\text{total}} \quad [1]$$

where t_{total} and Q were the time of exhaustion (min) and volumetric flow rate (mL/min).

The total adsorbed MB quantity q_{total} , in mg, (maximum column capacity) was expressed as:

$$q_{\text{total}} = \frac{QA}{1000} = \frac{Q}{1000} \int_{t=0}^{t=t_{\text{total}}} C_{\text{ad}} dt \quad [2]$$

where C_{ad} was the concentration of MB removal in mg/L. q_{total} represents the area below the breakthrough curve multiplied with the flow rate.

The amount of MB at equilibrium or biosorption capacity, q_e (mg of sorbated MB/g of biosorbent), was determined using the following equation,

$$q_e = \frac{q_{\text{total}}}{X} \quad [3]$$

where X is the mass of the biosorbent in g.

Various fixed bed models have been developed to predict the dynamic behavior of the column (16).

The Adams-Bohart model for rectangular isotherms

In the column mode, the adsorption kinetics for the MB can be presented by the Adams-Bohart model. It assumes a rectangular isotherm with a quasi-chemical rate expression. Axial dispersion and finite resistance to mass transfer are neglected in this model. The Adams-Bohart model (Eq. 4) is one of the most general and widely used models in the column performance theory. It is commonly, but mistakenly referred in the environmental sorption and biosorption literature as the Thomas model (17). The Adams-Bohart model in this paper was used, as follows:

$$\frac{C}{C_0} = \frac{1}{1 + \exp\left(\left(\frac{k_{\text{Th}}}{Q}\right)(q_0 X - C_0 V_{\text{eff}})\right)} \quad [4]$$

where k_{Th} is the rate constant (mL/min mg) and q_0 is the maximum solid-phase concentration of the solute (mg/g).



The Yoon-Nelson model

This model is based on the assumption that the rate of decrease in the probability of adsorption for each adsorbate molecule is proportional to the probability of adsorbate adsorption and the probability of adsorbate breakthrough on the adsorbent (11). In this work, the Yoon-Nelson model was used, as follows:

$$\ln\left(\frac{C}{C_0-C}\right) = k_{YN}t - \tau k_{YN} \quad [5]$$

where k_{YN} is the rate constant (1/min), τ the time required for 50% adsorbate breakthrough (min) and t is breakthrough time (min).

Clark model

This model combines the Freundlich isotherm and the mass transfer concept. The Clark model is presented in the following equations (18):

$$\left(\frac{C_0^{n-1}}{1 + \left[\left(\frac{C_0^{n-1}}{C_b^{n-1}} - 1 \right) e^{rt_b} \right] e^{-rt}} \right)^{\frac{1}{n-1}} = C \quad [6]$$

or

$$\left(\frac{1}{(1 + A e^{-rt})} \right)^{\frac{1}{n-1}} = \frac{C}{C_0} \quad [7]$$

where:

$$A = \left(\frac{C_0^{n-1}}{C_b^{n-1}} - 1 \right) e^{rt_b} \quad [8]$$

C_b , t_b and n are the outlet concentration at breakthrough, the time at breakthrough and the Freundlich constant, respectively.

Artificial neural network

Recently, traditional breakthrough curve models have been progressively replaced with artificial neural network (ANN) models. Witek-Krowiak et al. (19) summarized the studies that used ANN for modeling of batch and fixed bed biosorption process. The ANN predicts the output on the basis of the input data without the need to explicitly define the relationship between them, which is important in the complex process such as biosorption (20).



RESULTS AND DISCUSSION

Effect of the flow rate on the breakthrough curve

The effect of different flow rates on the shape of the breakthrough curves is shown in Figure 1. As can be seen, the breakthrough curves became steeper as the flow rate increased. The breakthrough time for reaching saturation increased with a decrease in the flow rate. It was found that at the lower flow rate, higher uptake values were observed for MB to maize stems. This phenomenon could be explained through a longer contact time of the MB with the adsorbent. Hence lower flow rates are desirable for the effective removal of MB.

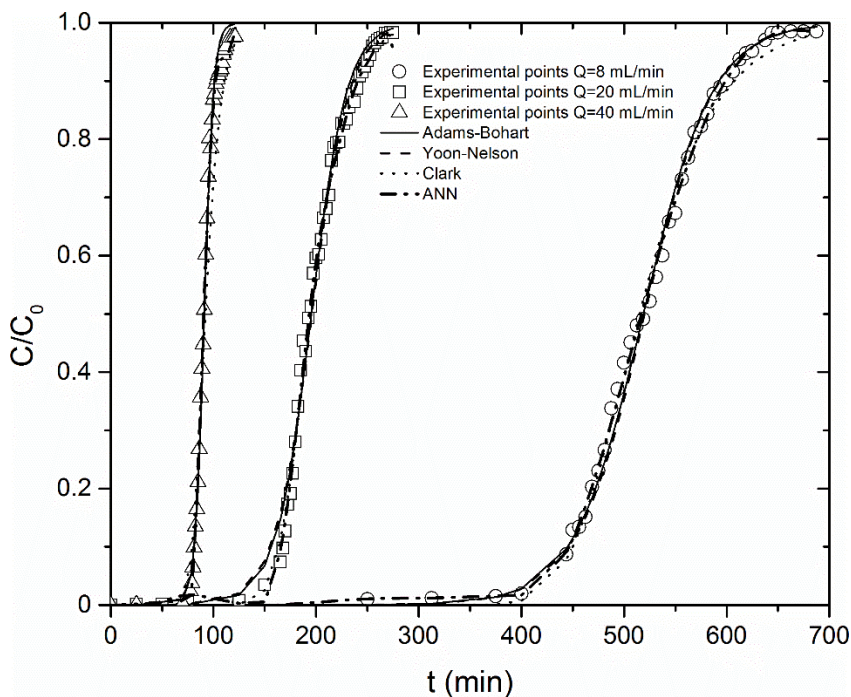


Figure 1. Comparison of the experimental and predicted curves obtained at different flow rates for $C_0 = 5 \text{ mg/L}$ and $Z = 6.5 \text{ cm}$

Effect of the influent MB concentration on the breakthrough curve

The adsorption performances of maize stems were tested at various initial concentration of MB (Figure 2). The breakthrough time decreased with the increasing inlet concentration as the binding sites became more quickly saturated in the system. Also, the



increase in the influent concentration resulted in a sharper breakthrough. The slope of the curve indicates high adsorption rates and shortened mass transfer zone.

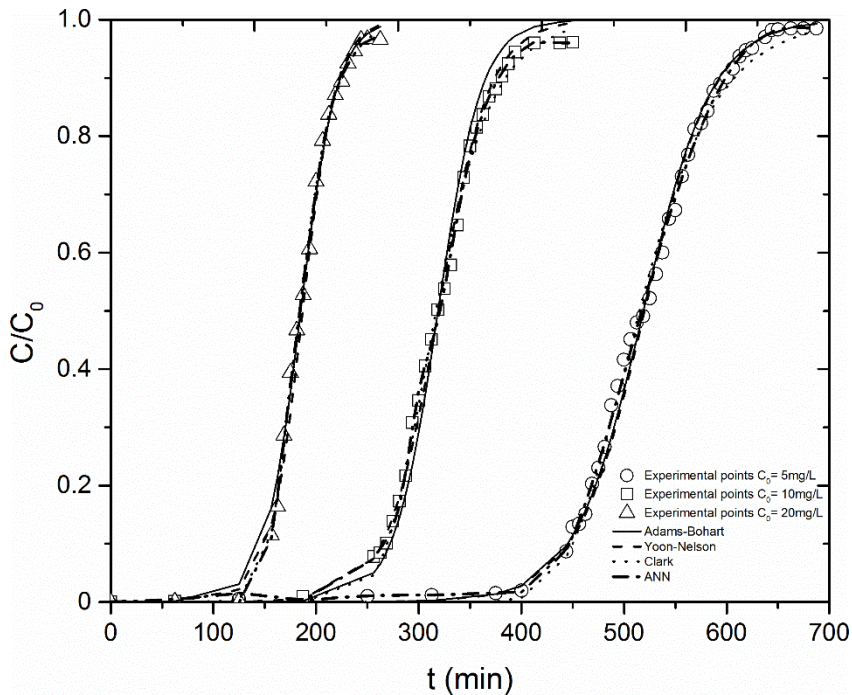


Figure 2. Comparison of the experimental and predicted curves obtained at different initial concentration for $Q = 8 \text{ mL/min}$ and $Z = 6.5 \text{ cm}$

The effect of the different bed depth on the breakthrough curve

The MB breakthrough curves, obtained from the experiments at different bed heights are presented in Figure 3. The figure shows that the breakthrough curve became steeper as the bed height decreased. The breakthrough times increased with the bed heights, thus allowing a larger volume to be treated. With a higher bed depth column, the mass transfer zone is extended and the MB had more time to be in contact with the adsorbent.

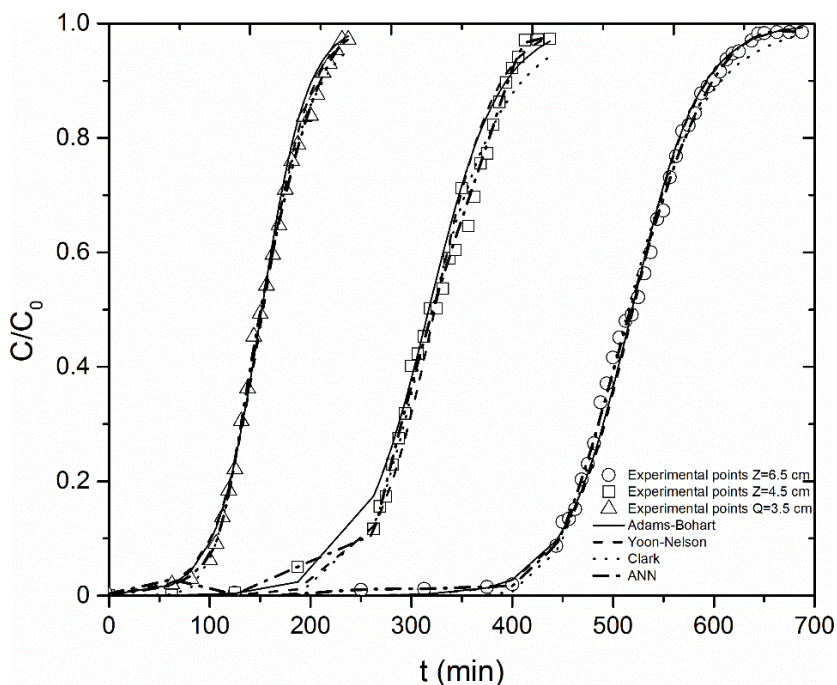


Figure 3. Comparison of the experimental and predicted curves obtained at different bed depth for $C_0 = 5 \text{ mg/L}$ and $Q = 8 \text{ mL/min}$

Error analysis

To describe the column breakthrough curves obtained at the different flow rates, MB inlet concentrations, and bed depths, three different models and ANN were used. The breakthrough curves showed the superposition of the experimental results (points) and the theoretically calculated points (lines). The coefficient of determination (R^2) shows a crude measure of how well a model describes the variation of the data. This is an intuitive, but crude, method to compare the two models, especially nonlinear models. In order to avoid this problem, an error analysis was performed according to the mean squared error (MSE). All models used in our paper have two unknown parameters, so in the discussion there is no need for complex error criteria that include the parameters of the models. The relative mathematical formula of MSE is:

$$MSE = \frac{\sum \left[\left(\frac{C}{C_0} \right)_e - \left(\frac{C}{C_0} \right)_c \right]^2}{n} \quad [9]$$

where $(C/C_0)_e$ is the ratio of the effluent and influent MB concentrations obtained from experiment and $(C/C_0)_c$ is the ratio of the effluent and influent MB concentrations



obtained from dynamic models, and n is the number of experimental data. Furthermore, the residual analysis of the developed model was also performed. The skewness parameters showed small deviations from a normal distribution, -1.37 to 2.34, while the kurtosis parameter showed a difference in "peakedness" compared to normal distribution, 2.83 to 7.21. However, the developed models showed statistically insignificant deviations from the experimental values of the model, which confirmed their suitability.

The Adams-Bohart model for the rectangular isotherm

The breakthrough curves (Figures 1-3) were described by the Adams-Bohart model for various experimental conditions. The Quasi-Newton method was used to evaluate the Adams-Bohart model parameters of k_{Th} and q_0 (Table 1).

Table 1. Parameters predicted from the Adams-Bohart model

C_0 (mg/L)	Q (mL/min)	Z (cm)	k_{Th} (mL/min mg ⁻¹)	q_0 (mg g ⁻¹)	R^2	MSE (10 ⁻³)	$q_e(\text{exp})$ (mg g ⁻¹)
5	8	6.5	5.95	31.92	0.99	0.51	31.88
10	8	6.5	4.73	39.23	0.99	1.62	39.33
20	8	6.5	2.85	45.57	0.99	0.56	45.93
5	20	6.5	11.61	30.07	0.99	1.02	30.45
5	40	6.5	43.94	28.04	0.99	0.87	28.22
5	8	4.5	5.7	28.19	0.99	2.07	28.65
5	8	3.5	8.84	24.25	0.99	0.71	24.56

It can be concluded from Table 1 that the increase in the initial concentration resulted in an increase in the value of q_0 and in a decrease in the value of k_{Th} . This is because the driving force for adsorption, i.e. the difference in the concentration of MB on the maize stems and in the solution, decreases with increasing initial concentration (21). The bed capacity q_0 slightly decreased, and the coefficient k_{Th} increased with increasing flow rate. Furthermore, with the increase in the bed volume, the value of q_0 increased. The Adams-Bohart model gave a bed capacity that was very close to the value determined in the batch process (15).

The Yoon-Nelson model

The Yoon-Nelson model was applied to investigate the breakthrough behavior of MB onto fixed bed of maize stems (Figures 1-3). The experimental breakthrough curves are very similar to those predicted by the Yoon-Nelson model. The values of k_{YN} and τ were determined using Quasi-Newton method and listed in Table 2. As is evident, the k_{YN}



increased and τ decreased with increasing both, flow rate and MB influent concentration. The increase in the bed volume caused an increase in τ and a decrease in k_{YN} .

Table 2. Parameters predicted from the Yoon-Nelson model

C_0 (mg/L)	Q (mL/min)	Z (cm)	k_{YN} (min ⁻¹)	T (min)	R ²	MSE (10 ⁻³)
5	8	6.5	0.018	475.75	0.99	0.59
10	8	6.5	0.015	232.54	0.99	0.42
20	8	6.5	0.033	161.14	0.99	0.85
5	20	6.5	0.052	195.48	0.99	0.98
5	40	6.5	0.099	79.48	0.99	0.82
5	8	4.5	0.033	322.51	0.99	2.03
5	8	3.5	0.044	157.05	0.99	0.44

The Clark model

The parameters of the Clark model and the determined coefficients for various conditions were obtained by the Levenberg-Marquardt model. The Freundlich constant n , obtained in our earlier batch equilibrium study, was used to calculate the remaining two parameters in the Clark model (15). The calculated parameters are given in Table 3. It is clear that if the flow rate and influent dye concentration increased, the value of r also increased. The determined coefficients and Figures 1-3 show a good agreement of the Clark model with the experimental data.

Table 3. Parameters predicted from the Clark model

C_0 (mg/L)	Q (mL/min)	Z (cm)	ln(A)	R (min ⁻¹)	R ²	MSE (10 ⁻³)
5	8	6.5	8.93	0.021	0.99	0.48
10	8	6.5	7.2	0.03	0.99	0.39
20	8	6.5	6.68	0.05	0.99	0.26
5	20	6.5	6.77	0.045	0.99	0.38
5	40	6.5	7.69	0.1	0.99	6.7
5	8	4.5	5.05	0.022	0.99	1.22
5	8	3.5	2.86	0.032	0.99	0.21



Artificial neural network

The feed-forward back propagation ANN was used to predict the experimental values for the breakthrough curve prediction. The Matlab neural network toolbox was used to build the ANN (The Math Works Inc. License Number 1108951). The ranges of the ANN inputs were: $0 < t < 687.5$, $5 < C_0 < 20$, $8 < Q < 40$ and $3.5 < z < 6.5$. In order to prevent the influence of the initial assumptions of weights and bias, the different topologies were used, in which the number of hidden neurons were varied from 1 to 20, and the training process of each network was run ten times with random initial values of weights and biases. The numbers of neurons were 13 and 1 in the hidden and the output layer, respectively (Figure 4). The network was trained using the Bayesian regulation back propagations algorithm. The others training algorithms (Levenberg-Marquardt, BFGS Quasi-Newton, Scaled Conjugate Gradient, etc.) were tested too, but they did not give satisfactory outputs. The transfer function was the linear transfer function (purelin) at the output layer, and the tangent sigmoid transfer function (tansig) at the hidden layer. All 235 data points were randomly used to train and develop the ANN; 70% of data points for training, 15% of data for validations, and 15% of data for testing the process. The optimum ANN topology was determined based on the MSE. The error analysis is shown in Table 4 for all experimental conditions.

Table 4. Error analysis for ANN

C_0 (mg/L)	Q (mL/min)	Z (cm)	R^2	MSE(10^{-4})
5	8	6.5	0.99	1.69
10	8	6.5	0.99	2.6
20	8	6.5	0.99	2.72
5	20	6.5	0.99	0.89
5	40	6.5	0.99	1.23
5	8	4.5	0.99	3.6
5	8	3.5	0.99	0.82

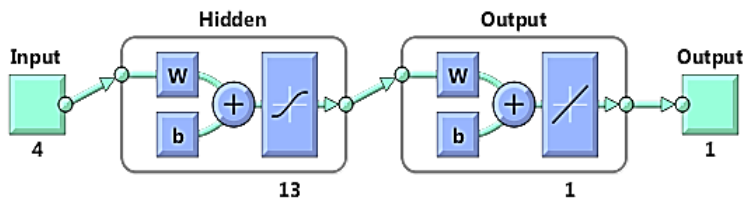


Figure 4. Topology of the ANN



CONCLUSIONS

The present study showed that the maize stems of Gold Cup could be used efficiently as a low cost and easily available biodegradable adsorbent for continuous removal of methylene blue from aqueous solutions.

The breakthrough curves showed that the breakthrough time increased with the increase in the bed height and with a decrease in the initial concentration and flow rate of methylene blue.

Three models and the artificial neural network were applied to the experimental data obtained from dynamic studies in order to predict the breakthrough curves and determine the column kinetic parameters. According to the MSE, the ANN model was the best fitting model compared to the Adams Bohart, Yoon-Nelson and Clark models. Further work needs to be done to establish the optimal conditions of flow rates, bed height, and initial methylene blue concentration to satisfy economic and technological requirements.

Acknowledgement

This research was supported by the Ministry of Education, Science and Technological Development of the Republic of Serbia. (Project No. 172025).

REFERENCES

1. Han, R.; Ding, D.; Xu, Y.; Zou, W.; Wang, Y.; Li, Y.; Zou, L. Use of rice husk for the adsorption of congo red from aqueous solution in column mode. *Bioresour. Technol.* **2008**, *99* (8), 2938-2946.
2. Gupta, V.K.; Suhas. Application of low-cost adsorbents for dye removal - A review. *J. Environ.Manage.* **2009**, *90* (8), 2313-2342.
3. Garg, V.K.; Amita, M.; Kumar, R.; Gupta, R. Basic dye (methylene blue) removal from simulated wastewater by adsorption using Indian Rosewood sawdust: a timber industry waste. *Dyes Pigm.* **2004**, *63* (3), 243-250.
4. McKay, G.; Porter, J.F.; Prasad, G.R. The Removal of Dye Colours from Aqueous Solutions by Adsorption on Low-cost Materials. *Water, Air, Soil Pollut.* **1999**, *114* (3), 423-438.
5. Otero, M.; Rozada, F.; Calvo, L.F.; García, A.I.; Morán, A. Kinetic and equilibrium modelling of the methylene blue removal from solution by adsorbent materials produced from sewage sludges. *Biochem. Eng. J.* **2003**, *15* (1), 59-68.
6. Kumar, K.V.; Ramamurthi, V.; Sivanesan, S. Modeling the mechanism involved during the sorption of methylene blue onto fly ash. *J. Colloid Interface Sci.* **2005**, *284* (1), 14-21.
7. Vadivelan, V.; Kumar, K.V. Equilibrium, kinetics, mechanism, and process design for the sorption of methylene blue onto rice husk. *J. Colloid Interface Sci.* **2005**, *286* (1), 90-100.



8. Han, R.P.; Wang, Y.F.; Han, P.; Shi, J.; Yang, J.; Lu, Y.S. Removal of methylene blue from aqueous solution by chaff in batch mode. *J. Hazard. Mater.* **2006**, *137* (1), 550-557.
9. Han, R.; Wang, Y.; Zhao, X.; Wang, Y.; Xie, F.; Cheng, J.; Tang, M. Adsorption of methylene blue by phoenix tree leaf powder in a fixed-bed column: experiments and prediction of breakthrough curves. *Desalination* **2009**, *245* (1-3), 284-297.
10. Rafatullah, M.; Sulaiman, O.; Hashim, R.; Ahmad, A. Adsorption of methylene blue on low-cost adsorbents: A review. *J. Hazard. Mater.* **2010**, *177* (1-3), 70-80.
11. Aksu, Z.; Gönen, F. Biosorption of phenol by immobilized activated sludge in a continuous packed bed: prediction of breakthrough curves. *Process Biochem.* **2004**, *39* (5), 599-613.
12. Bulut, Y.; Aydın, H. A kinetics and thermodynamics study of methylene blue adsorption on wheat shells. *Desalination* **2006**, *194* (1), 259-267.
13. Bhattacharyya, K.G.; Sharma, A. Kinetics and thermodynamics of Methylene Blue adsorption on Neem (*Azadirachta indica*) leaf powder. *Dyes Pigment.* **2005**, *65* (1), 51-59.
14. Bhatnagar, A.; Sillanpää, M. Utilization of agro-industrial and municipal waste materials as potential adsorbents for water treatment - A review. *Chem. Eng. J.* **2010**, *157* (2-3), 277-296.
15. Vučurović, V.M.; Razmovski, R.N.; Miljić, U.D.; Puškaš, V.S. Removal of cationic and anionic azo dyes from aqueous solutions by adsorption on maize stem tissue. *J. Taiwan Inst. Chem. Eng.* **2014**, *45* (4), 1700-1708.
16. Ruthven, D.M. *Principles of adsorption and adsorption processes*; John Wiley & Sons: 1984.
17. Chu, K.H. Fixed bed sorption: Setting the record straight on the Bohart-Adams and Thomas models. *J. Hazard. Mater.* **2010**, *177* (1-3), 1006-1012.
18. Clark, R.M. Evaluating the cost and performance of field-scale granular activated carbon systems. *Environ. Sci. Technol.* **1987**, *21* (6), 573-580.
19. Witek-Krowiak, A.; Chojnacka, K.; Podstawczyk, D.; Dawiec, A.; Pokomeda, K. Application of response surface methodology and artificial neural network methods in modelling and optimization of biosorption process. *Bioresour. Technol.* **2014**, *160*, 150-160.
20. Tovar-Gómez, R.; Moreno-Virgen, M.R.; Dena-Aguilar, J.A.; Hernández-Montoya, V.; BonillaPetriciolet, A.; Montes-Morán, M.A. Modeling of fixed-bed adsorption of fluoride on bone char using a hybrid neural network approach. *Chem. Eng. J.* **2013**, *228*, 1098-1109.
21. Chen, S.; Yue, Q.; Gao, B.; Li, Q.; Xu, X.; Fu, K. Adsorption of hexavalent chromium from aqueous solution by modified corn stalk: A fixed-bed column study. *Bioresour. Technol.* **2012**, *113*, 114-120.



КОНТИНУАЛНА АДСОРПЦИЈА БОЈЕ МЕТИЛЕНСКО ПЛАВО НА ПАРЕНХИМСКОМ ТКИВУ СТАБЛА КУКУРУЗА

*Предраг С. Којић**, *Весна В. Вучуровић*, *Наташа Љ. Лукић*, *Милица Ж. Караџић*,
Светлана С. Поповић

Универзитет у Новом Саду, Технолошки факултет Нови Сад,
Булевар цара Лазара 1, 21000 Нови Сад, Србија

У раду је испитана континуална адсорпција катјонске боје метиленско плаво на паренхимском ткиву стабла кукуруза у колони. Испитани су основни параметри који утичу на уклањање метиленског плавог из водених модел раствора а то су запремински проток и почетна концентрација адсорбата и висина слоја адсорбента. Максимални адсорпциони капацитет од 45,9 mg/g је остварен при почетној концентрацији метиленског плавог од 20 mg/L, висини слоја адсорбента од 6,5 cm и протоку од 8 mL/min. Установљено је да се време потребно за адсорпциону равнотежу повећава са смањењем запреминског протока и да се до равнотеже раније долази ако се повећа почетна концентрација адсорбата. Повећање висине слоја адсорбента омогућило је уклањање боје из веће запремине адсорбата. Модели Adams-Bohart-a, Yoon-Nelson-a и Clark-a као и вештачка неуронска мрежа су коришћени за предвиђање адсорпционих кривих. Ови модели су показали одлично слагање са експерименталним резултатима.

Кључне речи: биосорпција; адсорпциона крива; паренхимско ткиво стабла кукуруза; моделовање, неуронске мреже

Received: 04 September 2017.

Accepted: 13 October 2017.